JRC Scientific and Technical Reports

Modelling mesocosm experiments

Sibylle Dueri, Dimitar Marinov, José-Manuel Zaldívar, Morten Hjorth and Ingela Dahllöf

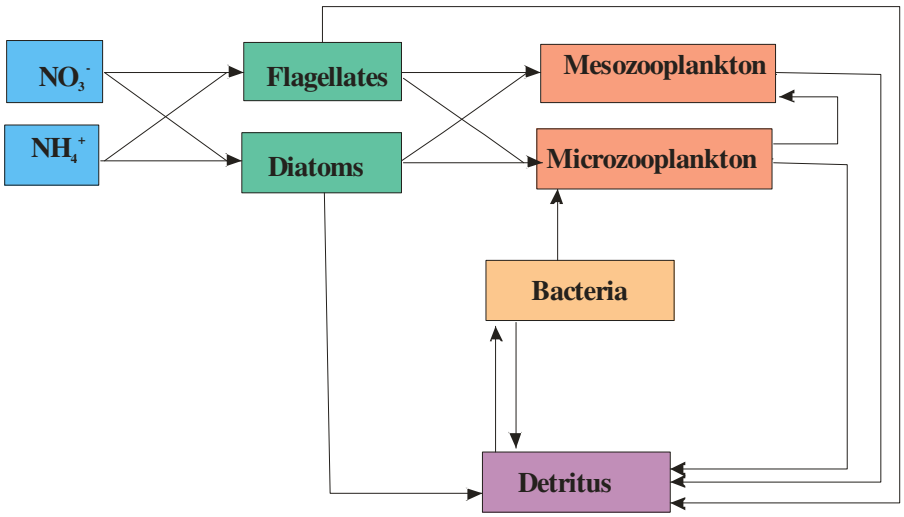

EUR 22952 EN - 2007

JRC
EUROPEAN COMMISSION

The mission of the Institute for Environment and Sustainability is to provide scientific-technical support to the European Union's Policies for the protection and sustainable development of the European and global environment.

European Commission
Joint Research Centre

Contact information
Address: Via E. Fermi 1, TP 272
E-mail: jose.zaldivar-comenges@jrc.it
Tel.: +39-0332-789202
Fax: +39-0332-785807

http://www.jrc.ec.europa.eu

JRC 40018

EUR 22952 EN
ISBN 978-92-79-07402-8
ISSN 1018-5593
DOI: 10.2788/3592

Luxembourg: Office for Official Publications of the European Communities

Printed in Italy

Table of Contents

List of Tables

List of Figures

1. Introduction

During the last decades coastal waters have been exposed to an increasing pressure of nutrients and contaminants related to agricultural, industrial and domestic activities. Input from rivers and effluents are one of the major sources of pollution in the coastal area from, but also inputs from atmospheric transport (dry and wet deposition and air-water exchange) can be a major contributor. Normally, a mixture of contaminants is present in transitional, coastal as well as marine waters, affecting their ecosystems.

The assessment of the combined effect of eutrophication and pollution on ecosystems is not straightforward due to complex interactions and feedbacks. Eutrophication may increase the primary production, dilute the contaminant in the biomass and furthermore increase the scavenging with the organic matter (Koelmans et al. 2001). On the other hand contaminants can have direct and indirect effects on the ecosystem balance and the growth of populations (Fleeger *et al*. 2003). Direct effects are caused by the toxicity of contaminants, which increase the mortality of the affected population; conversely indirect effects are the consequence of reduced food availability or reduced grazing. Thus, while nutrient acts on the bottom level of the food chain, contaminants may affect higher trophic levels and the correct understanding of the relative importance of top-down versus bottom-up controls is essential to evaluate the system.

The traditional approach for the modeling of contaminants in the water column is to consider two well-mixed boxes during stratification periods and one well-mixed the rest of the time (Schwarzenbach et al., 2003; Meijer et al., 2006). The extensive number of 0D models for hydrophobic organic compounds (Wania and Mackay, 1996; Scheringer et al., 2000; Dalla Valle et al., 2003; Dueri et al., 2005) contrasts with the lack of spatially and temporally resolved models, with the exception of the recently developed coastal lagoon model for herbicides (Carafa et al., 2006) and the one for HCH by Ilyina et al. (2006). A 1D dynamic hydrodynamic-contaminant model has been developed to analyze the influence of vertical mixing on the distribution of POPs in the water column (Jurado et al., 2007; Marinov et al., 2007). The model was applied to the organic contaminants families selected in Thresholds, i.e. PCBs, PAHs, and PBDEs, plus dioxins and furans, PCDD/Fs and details are presented in the Deliverable 2.6.2. Recently this 1D dynamic hydrodynamic-contaminant model was coupled with a food-web ecological model that considers phytoplankton, zooplankton, bacteria and detritus (Deliverable 2.6.3). The newly developed model uses nutrient concentrations as forcing and considers the bioaccumulation of POPs in all the ecological compartments. A first validation of the coupled model has been achieved using experimental data on PAHs obtained at the Finokalia Station, Island of Crete, Greece (Tsapakis et al., 2005 and 2006). The results showed that the model is able to reproduce the experimental concentrations as well as the measured fluxes. However, due to the low

concentrations of PAHs in the considered remote area environment, the toxic effect model could not be validated with those data.

Within the framework of the Threshold project, mesocosm experiments have been carried out in the Isefjord (Denmark) by NERI (Deliverable 4.3.3) to elucidate the combined effects of nutrient and pyrene on an ecosystem composed of phytoplankton, zooplankton and bacteria (Hjorth et al. 2007). The experimental results are used here to validate the model presented in Deliverable 2.6.3 on a smaller scale, including the toxic effect model and at the same time investigate the direct and indirect effects observed in the system.

2. Mesocosm experiments

A detailed description of the experimental work and its results is reported in Deliverable 4.3.3. The mesocosm experiments were carried out in the Isefjord (N: 55 42 44.4, E 11 47 28.51) between 23rd April and 4th May. The average depth of the fjord is 5-7 m. Twelve clear polyethylene cylindrical enclosures were filled with 3 m^3 ambient water and were attached 200 m from the shore. The bags were 2.5 m deep, and with a diameter of 1.25 m. The average temperature of measured in the bags during the experiments was between 10-15 ºC and the salinity was constant at 16 ppt. Sedimentation was avoided by gently pumping water from the bottom of the bags. Four different experiments were carried out:

1. Control experiment without any addition of nutrient or contaminant;
2. Enriched experiment with nutrient addition on day -1 and day 6; concentrations after addition: 4.8 µmol/L ammonia (NH_3Cl), 9.6 µmol/L silicate (Na_2SiO_3), 0.3 µmol/L phosphate (NaH_2PO_4) and ratio of 16:32:1 (N:Si:P);
3. Contaminant experiment with Pyrene addition (50nmol/L) on day 0 and day 7;
4. Experiment with contaminant and nutrient addition.

During the experiment different parameters were monitored: Chl a [µg/L], concentration of nutrients (Si, PO_4^{-3}PO4, NH_4^+, $NO_3^- + NO_2^-$) [µmol/L], primary production [dpm], bacterial activity [dpm] and copepod abundance [ind/L]. Also the distribution of 3 different communities of phytoplankton (2 flagellates and 1 diatom) was recorded by means of pigment analysis.

In addition to the experiments on the combined effect of nutrient and contaminants, another set of mesocosm experiments were carried out simultaneously in the Isefjord to observe the dynamics of attached microbial communities in an enriched system (Tang et al. 2006). Results from this study, which characterizes in detail the bacterial community and the zooplankton communities, were used to fit the bacterial part of the food web model and set the initial conditions of the micro- and mesozooplankton families.

3. Food web model

In order to simulate the toxic effects of contaminants in marine ecosystems as well as the effects of the biological pump on the dynamics of contaminants a simplified model has been developed. This model was considered as the minimum model able to deal with effects observed in the mesocosm experiments carried out by NERI (D.4.3.3). Deliverable D 2.6.3 describes the model's capabilities and features as well as the validation of the model using data of the Mediterranean Cruise and other campaigns. Hereafter we will summarize the main characteristics of the model.

The main compartments and interactions integrated in the model are represented in Fig. 3.1. The phytoplankton compartment is subdivided in two groups, diatoms and flagellates (*Pd, Pf*). Similarly, zooplankton has also been split into two groups representing microzooplankton (< 200 µm) and mesozooplankton (0.2-2 mm) (*Zs, Zl*). Moreover the microbial loop which accounts for the mineralization of dead organic matter, called detritus (*D*), performed by the bacteria (*B*), is incorporated in the model.

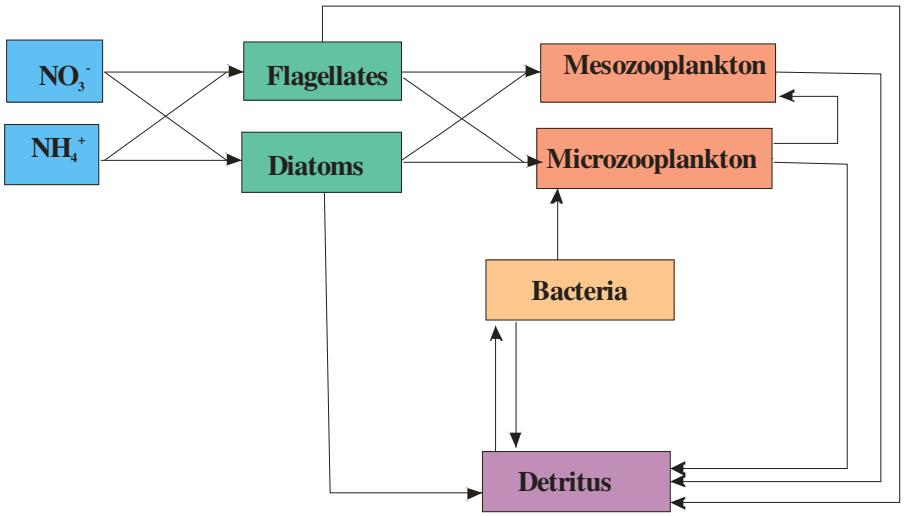

Figure 3.1. Simplified flow diagram in the marine ecosystem.

Nitrate and ammonium concentration in the water column are considered as forcing and therefore there is no dynamic interaction between the nutrient and the food web. The ordinary differential equations may be written as:

$$\frac{dPd}{dt} = growth_{Pd} \cdot Pd - grazing_{Pd}^{Zs} \cdot Zs - grazing_{Pd}^{Zl} \cdot Zl - m_{Pd} \cdot Pd \quad (1)$$

$$\frac{dPf}{dt} = growth_{Pf} \cdot Pf - grazing_{Pf}^{Zs} \cdot Zs - grazing_{Pf}^{Zl} \cdot Zl - m_{Pf} \cdot Pf \quad (2)$$

$$\frac{dZs}{dt} = \left(grazing_{Pd}^{Zs} + grazing_{Pf}^{Zs}\right) \cdot eff_P \cdot Zs + grazing_{B}^{Zs} \cdot eff_B \cdot Zs - grazing_{Zs}^{Zl} \cdot Zl - excre_{Zs} \cdot Zs - m_{Zs} \cdot Zs^2 \quad (3)$$

$$\frac{dZl}{dt} = \left(grazing_{Pd}^{Zl} + grazing_{Pf}^{Zl}\right) \cdot eff_P \cdot Zl + grazing_{Zs}^{Zl} \cdot eff_{Zs} \cdot Zl - excre_{Zl} \cdot Zl - m_{Zl} \cdot Zl^2 \quad (4)$$

$$\frac{dB}{dt} = growth_B \cdot B - kd_B \cdot B - grazing_B^{Zs} \cdot Zs \quad (5)$$

$$\frac{dD}{dt} = mort_{\det} + unassim_{\det}^{P} + unassim_{\det}^{Z} + unassim_{\det}^{B} - upt_B - \beta \cdot D - w_s \cdot D \quad (6)$$

3.1. Phytoplankton (*Pf* and *Pd* in mmol N m^{-3})

Phytoplankton growth is modelled as the product of the maximum specific growth rate times an overall limitation function as:

$$growth_{Px} = \mu_{\max}^{Px} \cdot \min[f_1(I), f_2(T), f_3(NO_3^-, NH_4^+)] \quad (7)$$

The light limitation is parameterized according to Jassby and Platt (1976) by

$$f_1(I) = \tanh[a_p \cdot I(z,t)] \quad (8)$$

$$I(z,t) = I_s \cdot \exp[-(k_{water} + k_{phy}[Pf + Pd]) \cdot z] \quad (9)$$

where a_p denotes the photosynthetic quantum efficiency parameter controlling the slope of *f(I)* versus the irradiance curve and I_s denotes the surface intensity of the PAR (photosynthetically active irradiance) taken as half of the incoming solar radiation. k_{water} is the extinction coefficient of the sea water and k_{phy} is the phytoplankton self-shading coefficient.

The temperature limitation function for phytoplankton is based on Lancelot *et al.* (2002)

$$f_2(T) = \exp\left[-\left(\frac{T - T_{opt}}{T_{width}}\right)^2\right] \quad (10)$$

with T_{opt} and T_{width} being the optimal temperature and the range of suitable temperatures respectively.

The nutrient limitation is the sum of ammonium and nitrate limitation:

$$f_3(NO_3^-, NH_4^+) = f_a(NO_3^-) + f_b(NH_4^+) \quad (11)$$

where the limitations are expressed by the Michaelis-Menten uptake formulation:

$$f_a(NO_3^-) = \frac{[NO_3^-]}{K_{no} + [NO_3^-]} \cdot \exp(-\psi[NH_4^=]) \quad (12)$$

$$f_b(NH_4^+) = \frac{[NH_4^+]}{K_{nh} + [NH_4^+]} \quad (13)$$

where K_{no} and K_{nh} are half saturation constants for nitrate and ammonium uptake, respectively, and the exponent in Eq. (12) represents the inhibiting effect of ammonium concentration on nitrate uptake with ψ=3 m^3 mmol N^{-1} (Wrobleski, 1977).

The mortality of phytoplankton is expressed as a linear function of its biomass.

3.2. Zooplankton (*Zs* and *Zl* in mmol N m^{-3})

In a similar way as in Oguz et al. (1999), we define the total food availability for each zooplankton group as:

$$F_{Zs} = b_{Pf} \cdot Pf + b_{Pd} \cdot Pd + b_B \cdot B \text{ and } F_{Zl} = a_{Pf} \cdot Pf + a_{Pd} \cdot Pd + a_{Zs} \cdot Zs \quad (14)$$

where a_{Pf}, a_{Pd}, a_{Zs} (0.3,0.8,0.7) and b_{Pf}, b_{Pd}, b_B (0.7,0.2,0.3) are the food preference coefficients. Grazing rates of microzooplankton are then defined as:

$$grazing_{Pd}^{Zs} = g_{\max}^{Zs} \frac{b_{Pd} \cdot Pd}{K_G + F_{Zs}} \quad (15)$$

$$grazing_{Pf}^{Zs} = g_{\max}^{Zs} \frac{b_{Pf} \cdot Pf}{K_G + F_{Zs}} \quad (16)$$

$$grazing_{B}^{Zs} = g_{maz}^{Zs} \frac{b_{B} \cdot B}{K_G + F_{Zs}} \quad (17)$$

where K_G is an apparent half saturation constant and $g_{\max}^{Zs}$ is the maximum grazing rate which is defined as a function of temperature as:

$$g_{\max}^{Zs} = g_{Zs}^{'} \exp\left[-\left(\frac{T - T_{opt}}{T_{width}} \right)^2 \right] \quad (18)$$

with T_{opt} and T_{width} being the optimal temperature and the range of suitable temperatures, respectively. The grazing of mesozooplankton is using the same type of equations.

Following Oguz et al. (1999) the mortality terms are expressed in the quadratic form as suggested by Steele and Henderson (1992). The assimilation coefficients eff_P, eff_{Zs} and eff_B are equal to 0.75.

3.3. Bacteria (B in mg C m^{-3})

Bacterial growth represents a fraction of detritus uptake:

$growth_B = Y_B \cdot upt_B$

and bacterial uptake is defined as:

$$upt_B = b_{\max} \frac{D}{K_D + D} B \quad (19)$$

where K_D is the half saturation value for detritus uptake and b_{max} is the maximum uptake rate of detritus by bacteria that depends on temperature as:

$$b_{\max} = b_{\max}^{'} \exp\left[-\left(\frac{T - T_{opt}}{T_{width}} \right)^2 \right] \quad (20)$$

3.4. Detritus (D in mg C m^{-3})

Phytoplankton, zooplankton and bacteria mortalities plus fecal pellets, constitute the unassimilated part of ingested food, contribute to the detritus compartment. Detritus due to mortality is expressed as:

$$mort_{\det} = \left(m_{Pd} \cdot Pd + m_{Pf} \cdot Pf\right) \cdot CN_P + \left(m_{Zs} \cdot Zs^2 + m_{Zl} \cdot Zl^2\right) \cdot CN_Z + kd_B \cdot B \quad (21)$$

where CN_P and CN_Z are ratios of mg C/mmol N for phytoplankton and zooplankton, respectively. CN_P=48, CN_Z =63. The other component consists on the unassimilated part of ingested food by zooplankton, that can be written as:

$$unassim^P_{\det} = (1 - eff_p) \cdot (grazing^{Zs}_{Pd} + grazing^{Zs}_{Pf}) \cdot Zs \cdot CN_P + (1 - eff_P) \cdot (grazing^{Zl}_{Pd} + grazing^{Zl}_{Pf}) \cdot Zl \cdot CN_P \quad (22)$$

$$unassim^Z_{\det} = (1 - eff_Z) \cdot grazing^{Zl}_{Zs} \cdot Zl \cdot CN_Z \quad (23)$$

$$unassim^B_{\det} = (1 - eff_B) \cdot grazing^{Zs}_{B} \cdot Zs \cdot CN_B \quad (24)$$

where CN_B is the ratio of mg C/mmol N for bacteria, CN_B=48. The other two terms in the mass balance for detritus account for the mineralization and for the settling, with a detritus decomposition rate β=4.17 10^{-3} h^{-1} and a sinking velocity w_s=8.33 10^{-2} m h^{-1}.

3.5. Toxic effect of contaminant

In the model the dose-response effects have been simulated using the Weibull equation:

$$f(x) = 1 - \exp[-\exp(\theta_1 + \theta_2 \log_{10} x)] \quad (25)$$

The mortality of the ecological compartments is changed as a function of the concentration of contaminant by adding to the mortality rate in the original equations, Eqs. (1)-(5), the induced pyrene mortality as given by Eq. (25). In addition this mortality term produces an increase in the detritus fraction and therefore a change in the distribution of the contaminant between dissolved and particulate phases.

3.6. Parameters, initial conditions and meteorological forcing of the mesocosm experiment simulation

The parameters of the food web model that have been used for the simulation of the mesocosm experiment are summarized in Table 3.1.

Initial concentration of phytoplankton was calculated from the Chl a concentration reported by in D 4.3.3 for the mesocosm experiment. Total concentration was partitioned between diatoms and flagellates according to the proportion observed in the system. Therefore in the simulation of the control experiment the initial concentration was set to 5 and 2.5 mmol N m^{-3} for the flagellates and the diatoms, respectively. Alternatively, in the enriched experiment they were set to 10 mmol N m^{-3} and 5 mmol N m^{-3}, respectively. The initial concentration of the large zooplankton compartment was defined according to the abundance of copepods at the beginning of the experiment, 3.5 ind L^{-1} . Taking a

mean carbon content per copepod of 2.5 µg C ind^{-1} (Van Nieuwerburgh et al. 2005) and converting to nitrogen the initial concentration of copepods corresponds to 0.14 mmol N m^{-3}. According to Tang et al. (2006), rotifers are the most abundant microzooplankton population and their mean abundance during the experiment was 106.3 ind L^{-1}. Taking a conversion coefficient of 0.6 µg C ind^{-1} (White and Roman 1992, Straile 1997) we obtain a mean concentration of rotifer of 1 mmol N m^{-3}. The initial value was set to half the mean value, corresponding to 0.5 mmol N m^{-3}. The initial concentration of bacteria was set to 10 mg C m^{-3} corresponding to the value measured at the beginning of the mesocosm experiment by Tang et al. 2006. Since data about the detritus concentration in the Isefjord is missing, it was estimated from the particulate organic carbon POC concentration measured in the Gullmar Fjord and Stretudden (Erlandsson et al. 2006) and was set to 200 mg C m^{-3}.

Table 3.1: Parameters used for the simulation of the mesocosm experiment.

Parameter	Definition	Value	Unit
a_p	Photosynthetis efficiency	0.01	$m^2\ W^{-1}$
k_{water}	Light extiction coefficient in sea water (coastal)	0.30	m^{-1}
k_{phy}	Phytoplankton self shading coefficient	0.08	$mmol\ N^{-1}$
$\mu max\ Pd$	Maximum growht rate for diatoms	0.03	h^{-1}
$\mu max\ Pf$	Maximum growht rate for flagellates	0.03	h^{-1}
$T_{opt,\ Pd}$	Optimal temperature for diatoms	10	ºC
$T_{opt,\ Pf}$	Optimal temperature for flagellates	15	ºC
$T_{width,\ Pd}$	Range of temperatures for diatoms	10	ºC
$T_{width,\ Pf}$	Range of temperatures for flagellates	10	ºC
K_{no}	Half saturation for nitrate uptake	2	$mmol\ N\ m^3$
K_{nh}	Half saturation for ammonium uptake	1	$mmol\ N\ m^3$
ψ	Ammonium inhibition parameter	3	$m^3\ mmol\ N^{-1}$
m_{Pd}	Diatoms mortality rate	0.0025	h^{-1}
m_{Pf}	Flagellates mortality rate	0.0025	h^{-1}
g_{Zs}'	Microzooplankton max grazing rate	0.050	h^{-1}
g_{Zl}'	Mesozooplankton max grazing rate	0.045	h^{-1}
$T_{opt,\ Zs}$	Optimal temperature for microzooplankton	14	ºC
$T_{opt,\ Zl}$	Optimal temperature for mesozooplankton	14	ºC
$T_{width,\ Zs}$	Range of temperature for microzooplankton	9	ºC
$T_{width,\ Zl}$	Range of temperature for mesozooplankton	9	ºC
K_G	Half saturation for zooplankton grazing	1.5	$mmol\ N\ m^{-3}$
m_{Zs}	Microzooplankton mortality rate	0.0022	h^{-1}
m_{Zl}	Mesozooplankton mortality rate	0.0024	h^{-1}
b'_{max}	Maximum uptake of detritus by bacteria	0.4	h^{-1}
K_D	Half saturation for detritus uptake by bacteria	25	$mg\ C\ m^{-3}$
$T_{opt,B}$	Optimal temperature for bacteria	30	ºC
$T_{width,B}$	Range of temperature for bacteria	18	ºC

The model also requires meteorological data for wind (speed and direction), humidity, cloud coverage, temperature and rainfall. The meteorological forcing is very important for the food web model, since primary production is highly influenced by temperature and radiation conditions. Data from a

meteorological station located 7 km from the study site was used for the simulations. Air temperature and radiation values used for the model are represented in Figure 3.2.

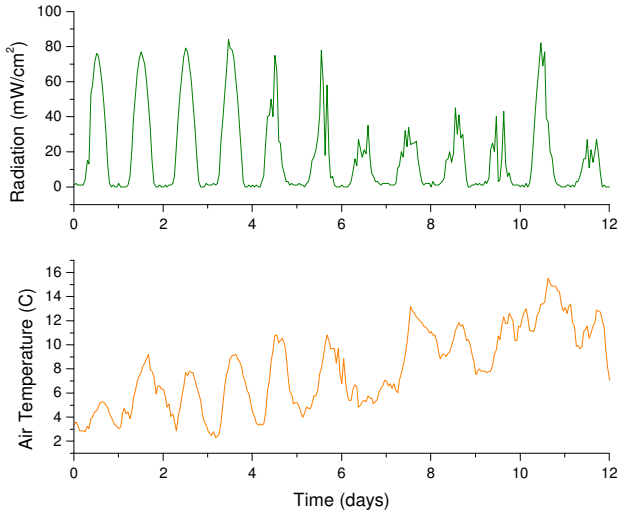

Figure 3.2: Sun radiation and temperature forcing used for the simulations.

4. RESULTS

4.1. Water Temperature

The hydrodynamic model simulates the temperature of the water column as a function of the meteorological forcing and the result is shown in Fig. 4.1. During the mesocosm experiment the water temperature was between 10 and 15 C which is in good agreement with the simulations.

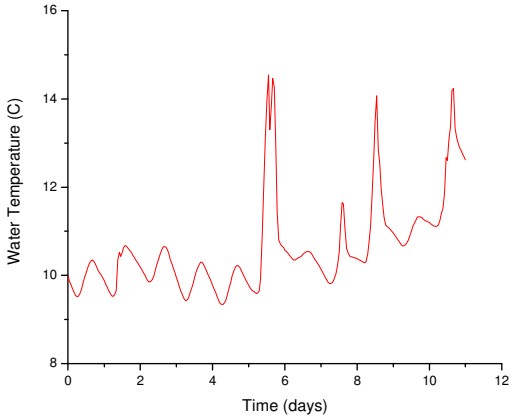

Figure 4.1: Simulated surface water temperature fluctuations during the mesocosm experiment

4.2. Control and enriched mesocosm `

The model was first calibrated for the control experiment, using the measured nitrate and ammonia concentration as forcing for the system (Fig. 4.2). The output is compared to the observed total

phytoplankton and copepod concentration, expressed in mmol N/ m3. (Fig. 4.3) and shows a reasonable fit to the observed decrease of the phytoplankton and the increase of the copepod population. However, in the simulation in the decrease phytoplankton population is initially delayed compared to the experiment.

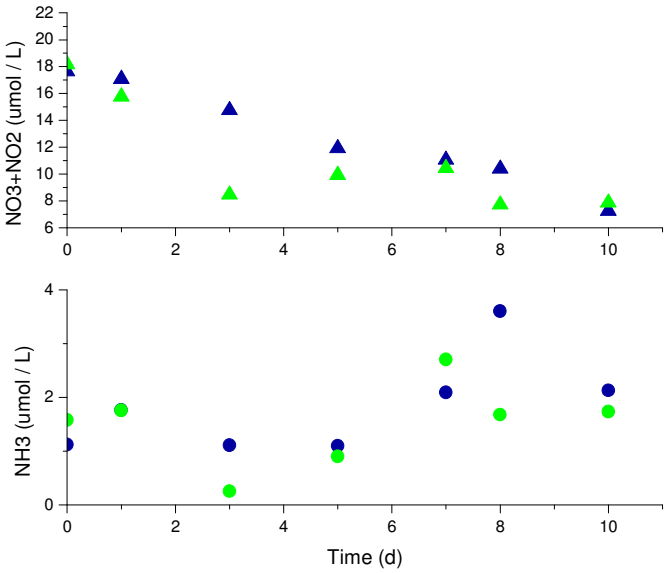

Figure 4.2: Observed nitrate and ammonia concentration in the control (blue) and enriched (green) mesocosm, used as forcing.

The simulations also show that the phytoplankton biomass is strongly regulated by the grazing of the zooplankton populations. The decrease of phytoplankton is almost parallel to the increase of the other population. In this sense the mesocoms seems to be strongly top-down regulated.

The simulation of the enriched mesocosm (Fig. 4.4) shows also an initial delay of the decrease of the phytoplankton population. In addition, the concentration of copepods at the end of the simulation is somewhat overestimated. In fact, in the experiments the concentration of copepods in the enriched mesocosm is lower than in the control, which is counterintuitive and the mechanism behind this observation is not clear. Moreover, it is interesting to remark that in both cases the simulation of the phytoplankton concentration shows a daily fluctuation related to the light limitation during the night.

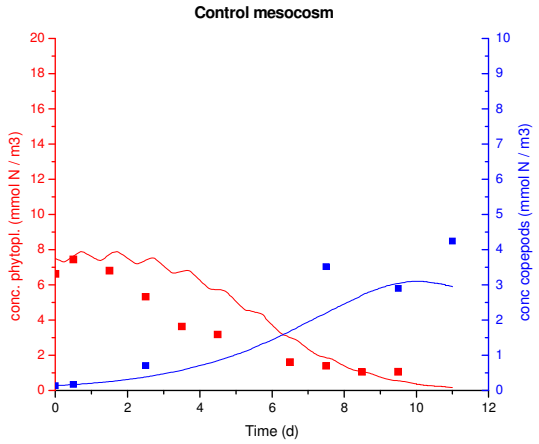

Figure 4.3: Comparison of the simulated values (line) with the observed values (points) for the control mesocosm

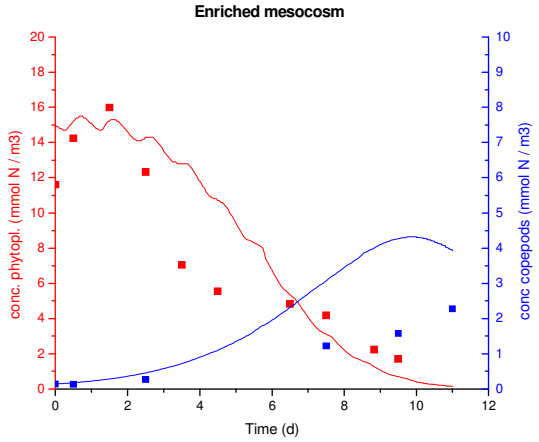

Figure 4.4: Comparison of the simulated values (line) with the observed values (points) for the enriched mesocosm.

The simulation of the ecological compartments (flagellates, diatoms, small and large zooplankton, bacteria and detritus) during the control and enriched experiments are shown in Figs. 4.5 and 4.6. Trends are similar for both runs. Microzooplankton grows faster than mesozooplankton, reaches a peak and decreases, while mesozooplankton reaches the peak only at the end of the simulation. The decline of diatoms is slower than the one of flagellates, due probably to different grazing and slower increase of their main predators, mesozooplankton. The decrease of the phytoplankton biomass is also related to an increase of the bacteria population, and in parallel a decrease of detritus.

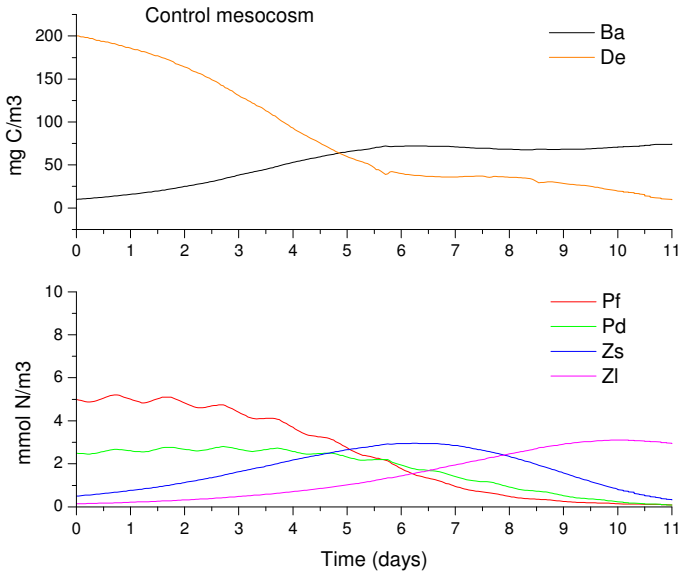

Figure 4.5: Simulation of the biomass and detritus distribution in the food web for the control mesocosm.

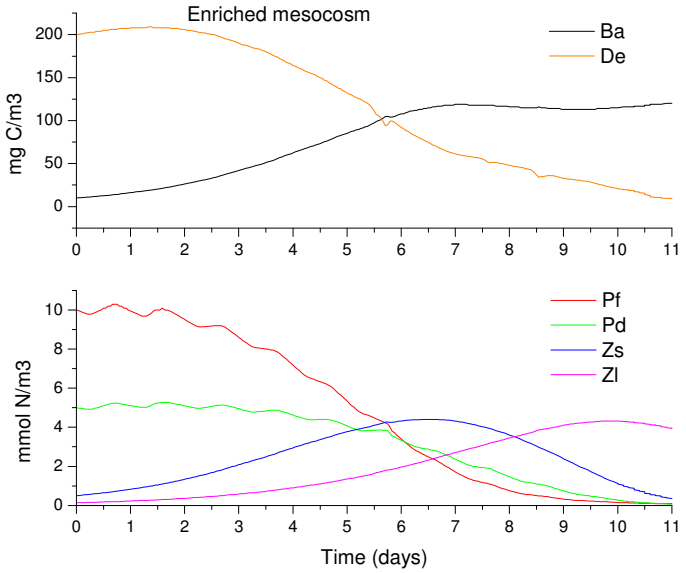

Figure 4.6: Simulation of the biomass and detritus distribution in the food web for the enriched mesocosm

4.3. Pyrene degradation

Data from the mesocosm experiment has highlighted that pyrene disappears very quickly from the system (Fig. 4.7). The model considers degradation, bioaccumulation and volatilization but none of those processes is able to cause such a rapid decline of pyrene. Therefore it was hypothesized that high

sorption of pyrene to the walls of the mesocosm bags is responsible for the observed trend. In order to account for the decrease of the contaminant concentration during the experiment, the degradation rate of pyrene was set to $4*10^{-5}$ s^{-1} meaning that half life of pyrene is about 5 hours. Compared to the degradation flux, volatilization flux is 2 orders of magnitude smaller.

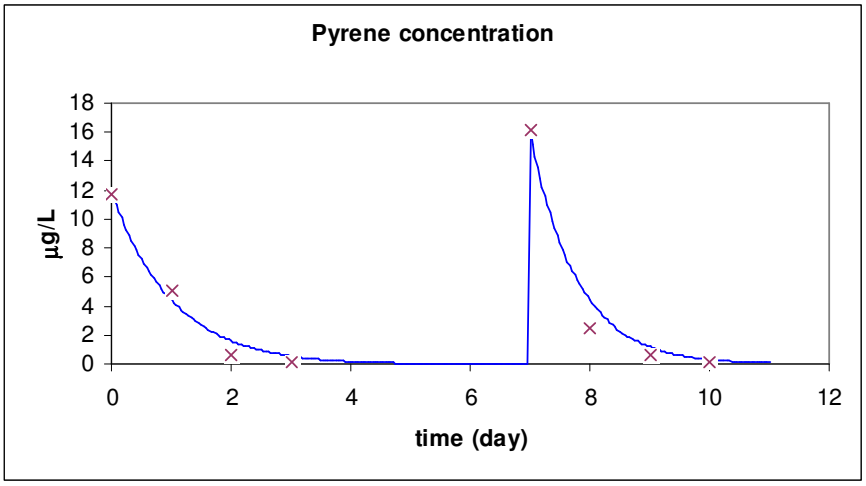

Figure 4.7: Observed (cross) and simulated (line) concentration of pyrene in the mesocosm

4.4. Toxic effects of pyrene in the mesocosm

In the model the toxicity of pyrene for each compartment of the food web model is described by the parameters θ_1 and θ_2 (Eq. 25), which define the shape of the dose-response curve (Fig. 4.8 and Table 4.1). For diatoms and flagellates the dose-response curve was fitted to data from the mesocosm experiment (D 4.3.3) and data from a study on phytoplankton communities in Greenland (Hjorth, 2005), while for zooplankton they were taken from an internet database http://www.pesticideinfo.org/ and other studies (Barata et al. 2005, Bellas and Thor, 2007). No data has been found for bacteria, therefore the toxicity data have been assumed low and comparable with unicellular species in the above mentioned database.

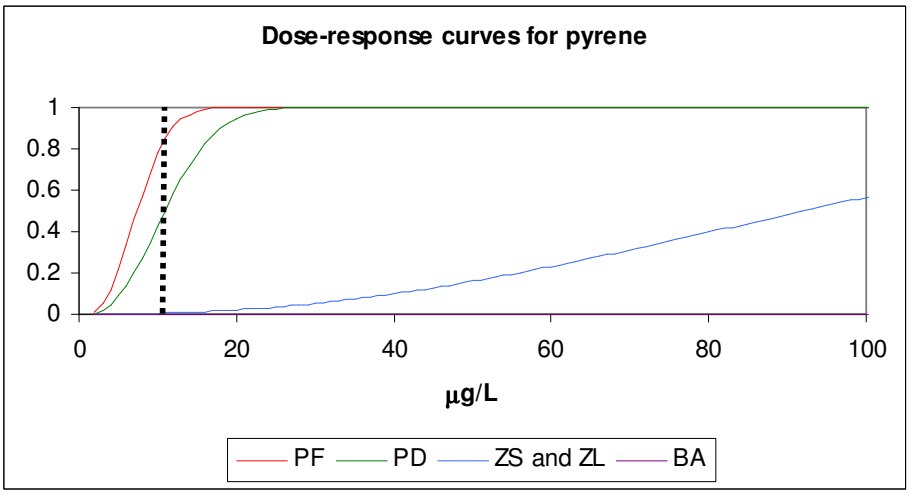

Figure 4.8: Dose-response curves used in the model. Dotted line represents the concentration of pyrene after addition.

Table 4.1. Parameters for the Pyrene dose-response function in the model.

Parameter	Phytoplankton: flagellates	Phytoplankton: diatoms	Zooplankton (both types)	Bacteria
θ_1	-4.5	-5.5	-10.442	-15.8486
θ_2	5.143	5.143	5.143	5.143

The simulation of the phytoplankton and mesozooplankton concentration after pyrene addition shows a reasonable fit with the observed values for both, the non-enriched and enriched system (Figures 4.9 and 4.10). Also in this case the simulated final concentration of copepods is slightly overestimated in the enriched system while in the non enriched system it is underestimated. Moreover the model predicts an important decrease of the phytoplankton population after the second addition of pyrene, while in reality the system shows a smooth decrease.

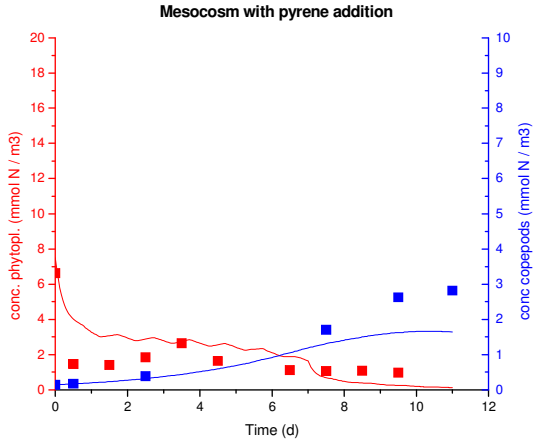

Figure 4.9: Comparison of the simulated values (line) with the observed values (points) for the mesocosm with pyrene addition

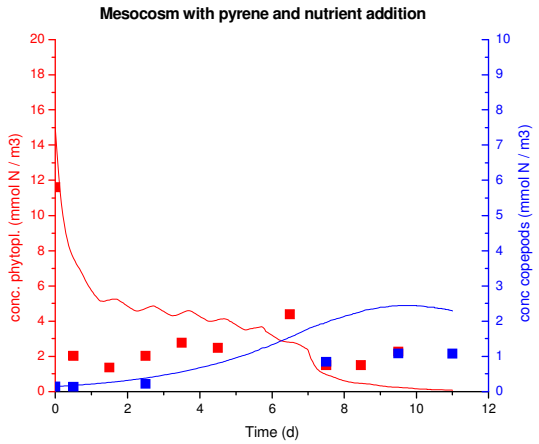

Figure 4.10: Comparison of the simulated values (line) with the observed values (points) for the enriched mesocosm with pyrene addition

The effect of pyrene addition depends on the sensitivities of the different species to the pollutant and the strength of indirect effects (Fig. 4.11). Flagellates are more affected than diatoms; therefore the relative abundance of diatoms increases during the simulation. Indirect effects are observed on the zooplankton growth, due to lower prey availability. The fast increase of detritus during day 1 and 2 is caused by the death of phytoplankton after addition of pyrene, in parallel there is a smooth increase of the bacteria population, which feeds on detritus. It is interesting to note that both addition of contaminant are followed by a peak in detritus production.

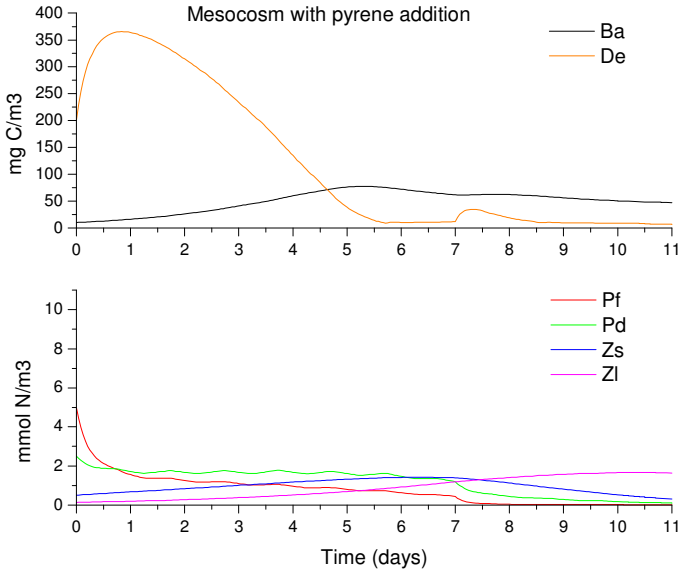

Figure 4.11: Simulation of the biomass and detritus distribution in the mesocosm with pyrene addition

Similar trends can be observed in the simulation of the enriched mesocosm (Fig. 4.12). According to the results of the mesocosm experiment, the effect of pyrene is stronger in the enriched mesocosm. Even though the concentration of phytoplankton is the double in the enriched system, after addition of pyrene it decreases to the same level as the non-enriched community. These observations were confirmed by the simulation results.

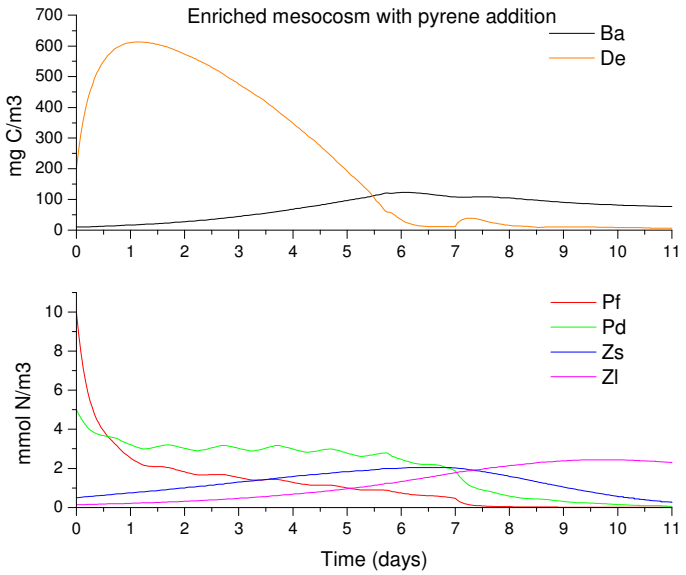

Figure 4.12: Simulation of the biomass and detritus distribution for the enriched mesocosm with pyrene addition.

5. DISCUSSION

The simulation succeeded well in representing the main direct and indirect effect observed in the mesocosm, like the stronger effect on the enriched community and there is a change in the phytoplankton composition due to higher toxicity for flagellates.

The simulation also highlighted that the results of the mesocosm depend on the natural conditions. Temperature and radiation influence the primary production, while the growth of zooplankton depends on the temperature and food availability, therefore choosing a different season for the experiment is likely to have a strong effect on the results. The system seems to be essentially top-down regulated and the decrease of phytoplankton in the control experiment is more likely to be caused by grazing than by reduced nutrient availability, since the system seems not to be limited by nitrogen concentration. On the other hand, the influence of enrichment was difficult to represent in the model, since the concentration of nutrient during the experiment was similar for the enriched and non-enriched mesocosm (Fig.4). Therefore in the simulations the main difference between the enriched and non enriched system were the initial phytoplankton concentration.

6. CONCLUSIONS

The outcome of the simulation highlighted some strengths and weaknesses of the methodology. On the one hand it showed that it is possible to represent the main dynamics observed in a mesocosm

experiment over a relatively short time (11 days) with a rather simplified food-web model. This confirms that the model contains the features necessary to represent the system correctly even on a small scale. On the other hand some of the parameters, e.g. the shape of the dose-response curve for phytoplankton and zooplankton, had to be fitted with a very limited amount of experimental data. More research is suitable in this field.

The difference between the enriched and non enriched communities was not that obvious to represent in the model, because the model considers only nitrogen and the data on $NO_3^- + NO_2^-$ and NH_4^+ concentrations in the enriched and non-enriched systems are similar. Since the experiments should represent environmentally reasonable enriched conditions, excessive nutrient additions had to be avoided. Further development of the model is required in order to represent the effect of nutrient addition under these conditions.

7. REFERENCES

Barata, C., Calbet, A., Saiz, E., Ortiz, L. and Bayona, J.M. 2005. Predicting single and mixture toxicity of petrogenic polycyclic aromatic hydrocarmobs to the Copepod Oithona davisae. *Environ. Toxic. Chem.* **24**(11) : 2992-2999.

Bellas, J. and Thor, P. 2007. Effects of selected PAHs on reproduction and survival of the calanoid copepod Acartia tonsa. *Ecotoxicology*, **16**(6):465-474.

Carafa, R., Marinov, D., Dueri, S., Wollgast, J., Ligthart, J., Canuti, E., Viaroli, P. and Zaldívar, J. M., 2006. A 3D hydrodynamic fate and transport model for herbicides in Sacca di Goro coastal lagoon (Northern Adriatic). *Mar. Poll. Bull*. **52**, 1231-1248.

Dalla Valle, M., Marcomini, A., Sfriso, A., Sweetman, A.J., Jones, K.C. 2003. Estimation of PCDD/F distribution and fluxes in the Venice Lagoon, Italy: combining measurement and modelling approaches.*Chemosphere* **51**, 603–616.

Dueri, S., Zaldívar, J.M. and Olivilla, A., 2005. Dynamic modelling of the fate of DDT in lake Maggiore: Preliminary results. EUR report n° 21663. JRC, EC. pp. 33.

Erlandsson C.P., Stigebrandt A. and Arneborg, L. 2006. The sensitivity of minimum oxygen concentrations in fjord to changes in biotic and abiotic external forcing. *Limnol. Oceanogr.* **51**(1): 631-638.

Fleeger, J.W., Carman, K.R. and Nisbet, R.M. 2003. Indirect effects of contaminants in aquatic ecosystems. *Sci. Tot. Environ.* **317**: 207-233.

Hjorth, M., Dahllöf, I. Forbes, V.E. 2007. Plankton stress responses from PAH exposure and nutrient enrichment. Sumbitted to *Mar. Ecol. Prog. Ser.*

Hjorth, M. 2005. Response of marine plankton to pollutant stress. Integrated community studies of structure and function. PhD Thesis. National Environmental Research Institute, Department of Marine Ecology/ Roskilde University, GESS, Denmark.32pp.

Ilyna, T., Pohlmann, T., Lammel, G., Sündermann, J., 2006. A fate of transport ocean model for persistent organic pollutants and its application to the North Sea. *J. of Mar. Systems* **63**,1–19.

Jassby, A. D. and Platt, T. 1976. Mathematical formulation of the relationship between photosynthesis and light for phytoplankton. *Limnol. Oceanogr.* **21**, 540-547.

Jurado, E., Zaldivar, J.M., Marinov, D. and Dachs, J. 2007. Fate of persistent organic pollutants in the water column: Does turbulent mixing matter? *Ma. Poll. Bull.* **54**, 441-451.

Koelmans, A.A., Van de Heijde, A., Knijff, L.M. and Aalderink, R.H. 2001. Integrated modeling of eutrophication and organic contaminant fate and effects in aquatic ecosystems. A review. *Wat.Res.* **35** : 3517-3536.

Lancelot, C., J. Staneva, D. Van Eeckhout, J.M. Beckers & E. Stanev, 2002. Modelling the Danube-influenced north-western continental shelf of the Black Sea. II. Ecosystem response to changes in nutrient delivery by the Danube river after its damming in 1972. *Estuarine and Coastal Shelf Science* **54**, 473-499.

Marinov, D., Dueri, S., Puillat, I., Zaldivar, J.M., Jurado, E. and Dachs, J. 2007- Description of contaminant fate model structure, functions, input data, forcing functions and physicochemical properties data for selected contaminants (PCBs, PAHs, PBDEs, PCDD/Fs) - EUR Report n 22627 EN.

Meijer, S.N., Dachs, J., Ferna´ndez, P., Camarero, L., Catalan, J., Del Vento, S., Van Drooge, B.L., Jurado, E., Grimalt, J.O., 2006. Modelling the dynamic air–water–sediment coupled fluxes and occurrence of polychlorinated biphenyls in a high altitude lake. *Environ. Poll*. **140**, 546–560.

Oguz , T., Ducklow, H. W., Malanotte-Rizzoli, P., Murray, J. W., Shushkina, E. A., Vedernikov, V. I. and Unluata, U. 1999. A physical-biochemical model of plankton productivity and nitrogen cycling in the Black Sea. *Deep-Sea Res.* I **46**, 597-636.

Scheringer, M., Wegmann, F., Fenner, K., Hungerbühler, K., 2000.Investigation of the cold condensation of persistent organic pollutants with a global multimedia fate model. *Environ. Sci. Technol.* **34**, 1842–1850

Schwarzenbach, R. P., Gschwend, P. M., Imboden, D. M., 2003, Environmental Organic Chemistry, 2nd Edition, Wiley Interscience, New York.

Steele, J. H. and Henderson, E. W. 1992. The role of predation in plankton models. *J. of Plankton Res.* **14**, 157-172.

Straile , D. 1997. Gross growth efficiencies of protozoan and metazoan zooplankton and their dependence on food concentration, predator-prey weight ratio, and taxonomic group. *Limnol. Oceanogr.* **42**(6), 1375-1385.

Tang K. W., Grossart, H.-P., Yam, E.M., Jackson, G.A., Ducklow, H.W. and Kiørboe T. 2006. Mesocosm study of particle dynamics and control of particle-associated bacteria by flagellate grazing. *Mar. Ecol. Prog. Ser.* **325**:15-27.

Tsapakis, M. and Stephanou, E. G., 2005. Polycyclic Aromatic Hydrocarbons in the Atmosphere of the Eastern Mediterranean. *Environ. Sci. Technol.*; **39**, 6584-6590.

Tsapakis, M., Apostolaki, M., Eisenreich, S., Stephanou, E. G., 2006. Atmospheric Deposition and Marine Sedimentation Fluxes of Polycyclic Aromatic Hydrocarbons in the Eastern Mediterranean Basin. *Environ. Sci. Technol.*, **40**, 4922-4927.

Van Nieuwerburgh, L., Wanstrand, I., Liu, J., Snoeijs, P., 2005. Astaxanthin production in marine pelagic copepods grazing on two different phytoplankton diets. *J. Sea Res.* **53**:147-160.

Wania, F., Mackay, D., 1996. Tracking the distribution of persistent organic pollutants. E*nviron. Sci. Technol.* **30**, 390A–396A.

White, J.R., and Roman, M.R., 1992. Seasonal study of grazing by metazoan zooplankton in the mesohaline Chesapeake Bay. Mar. Ecol. Prog. Ser. 86:251-261.

Wroblewski, J.A. 1977. A model of phytoplankton bloom formation during variable Oregon upwelling. *J. Mar. Res*. **35**, 357-394.

European Commission

EUR 22952 EN – Joint Research Centre
Title: **Modelling mesocosm experiments**
Author(s): Sibylle Dueri, Dimitar Marinov, José-Manuel Zaldívar, Morten Hjorth and Ingela Dahllöf
Luxembourg: Office for Official Publications of the European Communities
2007 – 25 pp. – 21 x 29,7 cm
EUR – Scientific and Technical Research series – ISSN 1018-5593
ISBN 978-92-79-07402-8

Abstract
In this report, an integrated model including fate of and effects of contaminants on an ecological model is presented. The aim is to simulate the dynamic behaviour of the mesocosm experiments carried out at NERI (see D431-D433) to elucidate the combined effects of nutrients and contaminants at ecosystem level. The outcome of the simulation highlighted some strengths and weaknesses of the methodology. On the one hand it is shown that it is possible to represent the main dynamics observed in a mesocosm experiment over a relatively short time (11 days) with a rather simplified food-web model. This confirms that the model contains the features necessary to represent the system correctly even on a small scale. On the other hand some of the parameters, e.g. the shape of the dose-response curve for phytoplankton and zooplankton, had to be fitted with a very limited amount of experimental data. More research would be necessary to elucidate this part of the model. The difference between the enriched and non enriched communities was not that obvious to represent in the model, since the data on $NO_3^- + NO_2^-$ and NH_4^+ concentrations in the enriched and non-enriched systems are similar.

The mission of the JRC is to provide customer-driven scientific and technical support for the conception, development, implementation and monitoring of EU policies. As a service of the European Commission, the JRC functions as a reference centre of science and technology for the Union. Close to the policy-making process, it serves the common interest of the Member States, while being independent of special interests, whether private or national.

JRC
EUROPEAN COMMISSION

LB-NA-22952-EN-C

ISBN 978-92-79-07402-8